In situ controlled heteroepitaxy of single-domain GaP on As-modified Si(100)

Oliver Supplie,[1,2,3,a] Matthias M. May,[1,2,3] Peter Kleinschmidt,[1] Andreas Nägelein,[1] Agnieszka Paszuk,[1] Sebastian Brückner,[1,2] and Thomas Hannappel[1,2,b]

[1]*Institut für Physik, Technische Universität Ilmenau, Gustav-Kirchhoff-Str. 5, 98693 Ilmenau, Germany*
[2]*Institute for Solar Fuels, Helmholtz-Zentrum Berlin für Materialien und Energie GmbH, Hahn-Meitner-Platz 1, 14109 Berlin, Germany*
[3]*Institut für Physik, Humboldt-Universität zu Berlin, Newtonstr. 15, 12489 Berlin, Germany*

(Received 6 July 2015; accepted 14 December 2015; published online 30 December 2015)

Metalorganic vapor phase epitaxy of III-V compounds commonly involves arsenic. We study the formation of atomically well-ordered, As-modified Si(100) surfaces and subsequent growth of GaP/Si(100) quasisubstrates *in situ* with reflection anisotropy spectroscopy. Surface symmetry and chemical composition are measured by low energy electron diffraction and X-ray photoelectron spectroscopy, respectively. A two-step annealing procedure of initially monohydride-terminated, (1×2) reconstructed Si(100) in As leads to a predominantly (1×2) reconstructed surface. GaP nucleation succeeds analogously to As-free systems and epilayers free of antiphase disorder may be grown subsequently. The GaP sublattice orientation, however, is inverted with respect to GaP growth on monohydride-terminated Si(100). © *2015 Author(s). All article content, except where otherwise noted, is licensed under a Creative Commons Attribution 3.0 Unported License.* [http://dx.doi.org/10.1063/1.4939005]

III-V heteroepitaxy on Si(100) in industrially scalable metalorganic vapor phase epitaxy (MOVPE) is highly desirable for high-efficiency opto-electronic devices. In general, a detailed understanding of MOVPE growth processes is complicated by the presence of a process gas, various precursors, their fragments, and reactor residuals from previous growth runs, as well as the competition between kinetically and energetically driven processes at elevated temperatures. Regarding III-V-on-silicon, polar-on-nonpolar epitaxy adds further complexity.[1] Defect-free, pseudomorphic GaP/Si(100) quasisubstrates, where the transition from nonpolar silicon to polar GaP is already achieved, are ideally suited for further III-V growth, either lattice-matched[2,3] or metamorphic.[4] For such quasisubstrates, both single-domain Si(100) substrate preparation[5–7] and adequate sequences of pulsed GaP nucleation and GaP growth[8–16] must be controlled precisely. The electronic properties across the interface, such as band offsets, are highly influenced by its atomic structure. Single-domain Si(100) surfaces suppress antiphase disorder completely, which is favorable over annihilation of antiphase boundaries[12] in case the Si(100) substrate is used as active part of the device.

Arsenic termination of Si(100) is beneficial for III-V heteroepitaxy as it was found to hinder out-diffusion of Si into the GaP epilayer.[17] The influence of arsenic on GaP/Si(100) heterointerface formation and GaP epilayer growth, however, has been studied much less compared to As-free GaP nucleation, even though As is mostly present in MOVPE growth process ambient, either as As_4 stemming from background residuals or in form of a precursor.

In UHV, it is known that As_4 highly impacts the atomic order at clean Si(100) surfaces, which, in turn, influences subsequent GaAs heteroepitaxy.[18,19] Depending on processing routes, As dimers

[a]Electronic mail: oliver.supplie@tu-ilmenau.de
[b]Electronic mail: thomas.hannappel@tu-ilmenau.de

were found to bond either additive or replacive with respect to the Si dimers of the As-free surfaces. Dimerized terraces with predominant (1×2) reconstruction (also called A-type, T_A) and with predominant (2×1) reconstruction (also called B-type, T_B) could be achieved.[19] In consequence, the sublattice orientation of subsequently grown GaAs can be inverted.[18] In contrast to background As_x, both arsine (AsH_3) and tertiarybutylarsine (TBAs) were found to etch Si(100) surfaces in MOVPE ambient.[20–22] Supply of TBAs or AsH_3 during thermal deoxidation of the Si substrate was found to decrease the required temperatures below 900 °C.[20–22] These TBAs-annealed Si(100) surfaces showed a two-domain surface structure[21] which would result in antiphase disorder in III-V epilayers.[1]

Here, we studied the preparation of Si(100) and subsequent GaP heteroepitaxy *in situ* in presence of arsenic. *In situ* reflection anisotropy spectroscopy (RAS) and benchmarking to low energy electron diffraction (LEED), scanning tunneling microscopy (STM), and X-ray photoelectron spectroscopy (XPS) allow for preparation and control of well-defined Si(100) surfaces in MOVPE ambient which is crucial for understanding the GaP/Si interface formation. Therefore, we used Si(100) with 2° misorientation towards [011], where it is possible to form stable predominantly A-type terraces similar to our results in the As-free H_2 ambient.[6] A two-step annealing process of A-type Si(100) in As was applied to form an As-modified Si(100) surface with A-type terraces. We investigated the influence of the Si surface preparation and termination on the interface formation and sublattice orientation of subsequently grown GaP.

All samples were prepared in a horizontal AIX-200 MOVPE reactor (Aixtron), which is modified with a dedicated MOVPE-to-UHV transfer system.[23] Preparation of the Si(100) 2° surfaces is described in detail in Ref. 6. Process temperatures were measured with a thermocouple placed in the susceptor. The reactor contained (Ga,P,As) background residuals from previous growth runs. Throughout the entire process, changes of the atomic order at the surfaces were monitored *in situ* with RAS, an optical technique particularly sensitive to asymmetrically reconstructed (100) surfaces of cubic crystals.[24] RAS (LayTec EpiRAS-200) was aligned such that the difference in reflection along $[0\bar{1}1]$ and [011] was measured with intensities normalized to the Si(110) standard.[24] Selected samples were transferred contamination-free to UHV,[23] where symmetry and chemical composition of the surface were measured by LEED (Specs ErLEED 100-A), STM (Specs 150 Aarhus), and XPS (Specs Focus 500 and Phoibos 150), respectively.

Fig. 1(a) shows a RAS contour plot, where RA spectra of Si(100) were measured continuously with colorcoded amplitude during a two-temperature annealing procedure in TBAs and background As, respectively. Arrows mark spectra of Si(100) prior and after As-modification of the surface, which are juxtaposed in Fig. 1(b). Before offering any III-V precursor, we applied the process established for formation of A-type terraces[6] and cooled to 420 °C. The corresponding RAS signal (green, dashed-dotted line) shows the well-known lineshape of Si(100) with predominantly A-type terraces, where monohydride-terminated Si dimers are aligned in rows in parallel to the step edges.[6,26] Consequently, this surface can also be prepared in MOVPE processing ambient, where As (and Ga, P) was involved in previous processes. The amplitude of the RAS signal here implies a T_A:T_B domain imbalance of about 7:3.[6,26] For preparation of the As-modified Si(100) surface, TBAs is offered at 420 °C. The dielectric anisotropy changes drastically: A broad peak centered at about 3.7 eV (labelled A_1) emerges and the Si dimer related minimum peak at E_1 has almost vanished. Despite a temperature related shift and decrease in amplitude,[27] these features persist when heating to 670 °C under continuous TBAs supply. A contribution below the E_1 interband transition of Si (A_2) slowly increases during continuous annealing at 670 °C. The spectrum is not yet comparable to that of Si(100) terminated with As dimers.[19,21,22] Therefore, we continued annealing at higher temperatures. Since TBAs is known to etch Si(100) at elevated temperatures,[20,22] we turned off the TBAs supply (background As_x is present). The RAS signal does not change at first (apart from temperature effects on the optical transitions). A_1, however, seems to sharpen beyond about 800 °C and, simultaneously, a second local minimum becomes apparent at about 4 eV (A_3). Reaching 850 °C, both A_2 and A_3 increase rather suddenly in amplitude and remain stable at 850 °C. During cooling, A_1, A_2, and A_3 exhibit differently pronounced temperature-dependent energetic shifts.[27] At 420 °C, the RA spectrum (orange line, abbreviated Si-As) clearly shows A_2 about 100 meV below E_1^{Si}, A_1 of similar amplitude at 3.7 eV as well as A_3 at 4.1 eV and a broad contribution below 2.7 eV (A_4). The lineshape of the RA spectrum of the final As-modified Si(100) surface shows now more

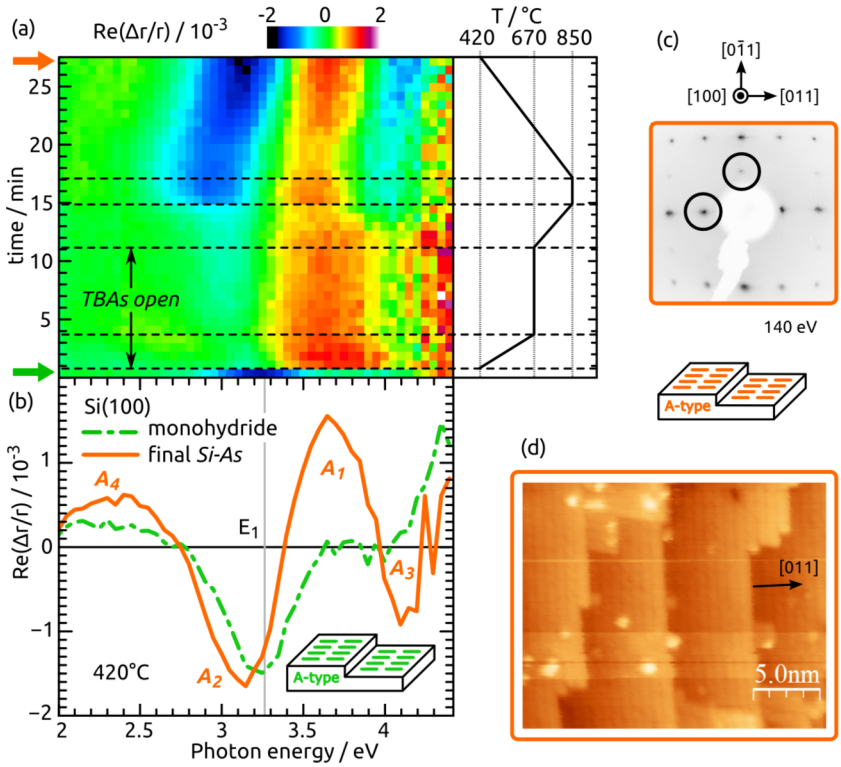

FIG. 1. (a) RAS contour plot of Si(100) with 2° misorientation towards [011] in H_2 at temperatures indicated at the right hand side. The black arrow marks TBAs supply and bold green/orange arrows mark the RA spectra of monohydride-terminated and As-modified Si(100), which are compared in (b). The vertical gray line indicates the E_1 transition of Si.[25] (c) LEED pattern of a Si-As sample. Circles mark spots at half order. Insets indicate the majority dimer orientations with respect to the step edges according to LEED. (d) STM image (empty states) of a Si-As sample.

similarity to that of As-terminated Si(100) prepared by additive As_4 adsorption on B-type Si(100) with 4° misorientation towards [011] in UHV.[19] Except for a scaling factor, also As-terminated Si(100) surfaces prepared in MOVPE ambient[21,22] showed comparable RA spectra to those prepared in UHV. The Si-As surface measured here, however, exhibits more intense peaks compared to the UHV-prepared sample.[19] A_2, in particular, is more than twice as intense. While Kipp *et al.*[19] claim a domain ratio of T_A:T_B = 9:1 for the UHV-prepared samples, Bork *et al.*[21] refer to LEED showing two-domain patterns after TBAs annealing in MOVPE ambient. Both surfaces are believed to be terminated with one monolayer (ML) As.[19,21] The LEED pattern of a Si-As sample in Fig. 1(c) shows a high domain imbalance towards T_A, as indicated by the strong spots at half order along [011] direction. Fig. 1(d) depicts a STM image of a Si-As sample, where both terrace width and step height correspond to a double-layer stepped surface. A-type dimer rows are clearly visible. Single-, double-, and triple-layer steps were most prominent and no significant step bunching was observed.

After As-modification, As is present at the surface as verified by XPS measurements of the As $2p_{3/2}$ photoemission (PE) line displayed in Fig. 2. The bigger component As_1 most probably stems from Si–As bonds, which agrees with the occurrence of two components in the Si 2p PE line, Si_1 and Si_2 (the ratio of $2p_{3/2}$ and $2p_{1/2}$ was fixed to 2:1 and 0.61 eV was used for the spin-orbit splitting for fitting the measured data). We did not detect any typical contaminants, such as O, C, or Ga, on the surface, which implies that one of the contributions is chemically shifted by incorporated As atoms. The relative contribution of the Si_2 component increases when the photoelectron takeoff angle (with respect to surface plane) is varied from 90° (Fig. 2(b)) to 30° (Fig. 2(c)). This indicates that Si_2 is a (near) surface component, while the Si_1 signal stems rather from the bulk. The $2p_{3/2}$ components of Si_1 and Si_2 are located at binding energies (E_B) of 99.34 eV and 99.72 eV, respectively. A chemical shift of Si_2 towards higher E_B would also be expected assuming Si–As bonds.[28]

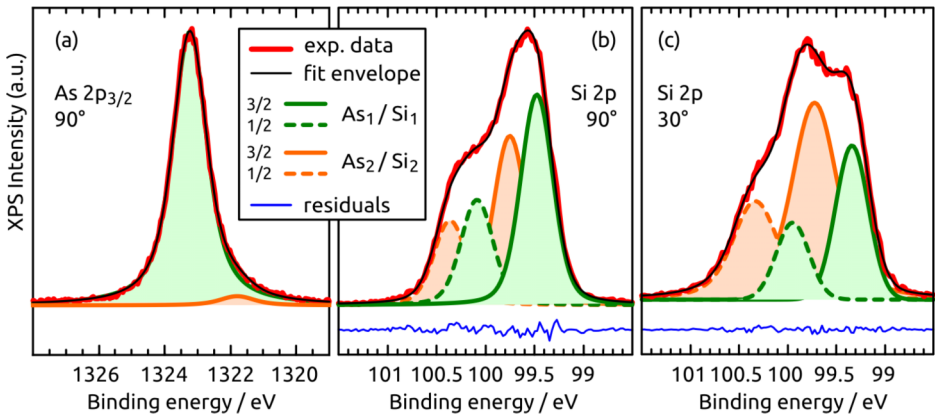

FIG. 2. XPS data (red lines) of (a) As $2p_{3/2}$ and ((b) and (c)) Si 2p PE lines of As-modified Si(100), which were measured ((a) and (b)) at 90° and (c) at 30° photoelectron takeoff angle. The fit envelope (black line) and its components (As_1/Si_1, green line; As_2/Si_2, orange line; solid for 3/2 and dashed for the 1/2 components) are indicated. Monochromated Al K_α excitation was used and E_B is given with respect to E_F.

A quantitative estimation[29] of As on the surface via the As 2p peak—under the assumption of a fractional coverage and an abrupt interface—roughly reveals a coverage of 0.75 ± 0.5 ML of As. Given the photoelectron escape depth of several nm, the high intensity of Si_2, however, indicates that a simple model of one single As monolayer on top of a continuous Si bulk fails here. Probably, intermixing occurs at the interface, which impedes precise quantification of the amount of As being present.

Referring to calculated RAS signals, Kipp *et al.*[19] ascribed the spectral features of As-terminated Si(100) to (i) electronic transitions between surface modified bulk states and antibonding As dimer states and (ii) to transitions between bonding and antibonding As dimer states. However, their calculations do not reproduce A_2, which is assigned to Si–As bonds and As lone pairs.[30] According to RAS (Fig. 1), monohydride-terminated Si(100) was prepared here prior to As-modification. Since H was found to limit As adsorption,[31] the formation of A_2 at temperatures above 800 °C could be related to an increase in H desorption rates facilitating replacement of Si by As present in the reactor. This would, however, not explain the early appearance of A_1, which suggests different origins of A_1 and A_2. During annealing at 850 °C, As will also desorb from the surface.[32] This explains the slight decrease of the RAS amplitude in Fig. 1 when the cooling starts and can be verified during longer annealing at 850 °C in case the amount of background As is insufficient to compensate As desorption.

For the monohydride-terminated Si(100) surface, the amplitude of the RAS peak at 3.4 eV reflects the domain ratio at the surface.[6,26] Possibly, the RAS signal of Si-As contains contributions from As dimers and monohydride-terminated Si dimers, both with majority T_A domains, which is represented in the amplitude of A_2. The surface formation of Si(100) in H_2 is complex in this temperature range due to the competition of a kinetically driven step formation triggered by H_2 interaction and the influence of As (additive vs. replacive adsorption[18]). Simple additive As adsorption, however, can be excluded due to the prevalent (1×2) reconstruction of Si-As. Further benchmarking[33] of the Si(100) surface prior to heating in background arsenic will be performed for a detailed understanding of the As incorporation.

In situ RAS enables us to prepare a very well-defined Si(100) surface prior to GaP nucleation featuring A-type terraces either terminated with H or modified with As, which we will use in the following to compare the interface formation of GaP heteroepitaxy on Si-As with previous results of GaP grown on monohydride-terminated Si(100).[15] After GaP growth, the P-rich $(2 \times 2)/c(2 \times 4)$ reconstructed surface was prepared. The RMS roughness measured by atomic force microscopy typically is on the order of 5 Å. The RAS signal of such a surface is related to its buckled P dimers.[35,36] In case of GaP/Si(100) heteroepitaxy, the lineshape of the RAS signal results from a convolution of the GaP(100) surface dielectric anisotropy, thickness dependent interference, and the dielectric

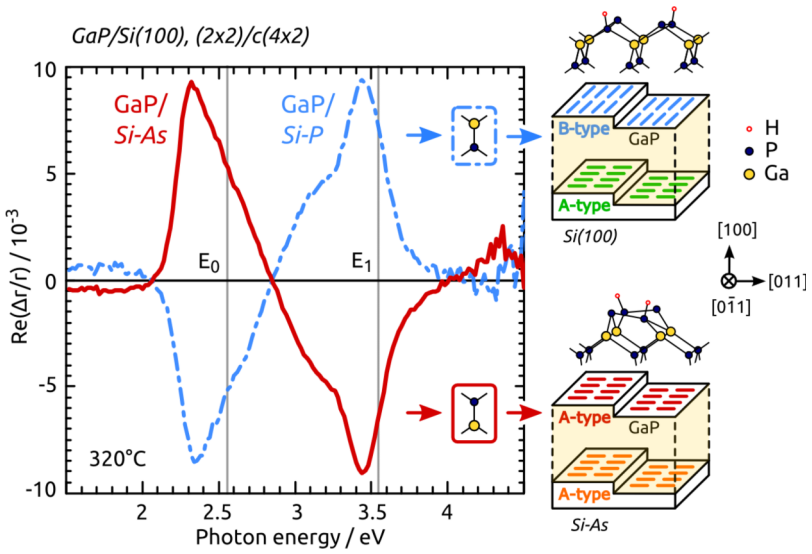

FIG. 3. RAS of P-rich, $(2\times2)/c(4\times2)$ reconstructed surfaces of about 40 nm thick GaP epilayers grown on Si-As (red line) and monohydride-terminated Si(100) (GaP/Si-P, dashed-dotted blue line). Vertical lines indicate interband transitions of GaP.[34] Insets on the right indicate corresponding dimer orientations at the substrate prior to nucleation and at the GaP/Si surface, respectively (top for GaP/Si-P, bottom for GaP/Si-As). Barbell-like structures (red, respectively, blue box) indicate the sublattice orientation deduced from the orientation of the P dimers shown atop the insets.

anisotropy of the buried heterointerface.[16] Given the tetrahedral coordination of the zincblende lattice, the sublattice orientation of the GaP epilayer defines the P dimer orientation.[15] The latter can be measured by the sign of the GaP/Si(100) RAS signal.[37] Fig. 3 compares the RA spectrum of GaP/Si-As (red line) to that of GaP grown on monohydride-terminated Si(100) (GaP/Si-P, blue dashed-dotted line). Despite the sign, the lineshape is almost identical, which implies that the GaP layer thickness is comparable and that the GaP/Si-As surface is atomically as well ordered as the GaP/Si-P reference surface. The sign of the RA spectrum of GaP/Si-As corresponds to P dimers aligned in rows parallel to $[0\bar{1}1]$ direction (A-type), as shown in the inset in Fig. 3. This implies an inverted GaP sublattice of GaP/Si-As compared to GaP/Si-P, as indicated in the ball-and-stick model in Fig. 3.[15] This inversion is induced by the GaP/Si-As heterointerface. Considering the T_A surface prior to nucleation in a simplified model,[14,15] either Ga would bind first on top of Si-As or P atoms replace the dimer layer of Si-As during nucleation. However, given the high intensity of the Si-As XPS signal (Fig. 2), the interface is probably more complex than the abrupt Si–P interface prepared by pulsed GaP nucleation on monohydride-terminated Si(100).[16] Preliminary XPS measurements of the Si 2p PE line after GaP nucleation reveal that a third Si component emerges (not shown here), which implies that Ga is not simply binding to As on top of Si at an abrupt interface. Since antiphase disorder would result in surface domains of mutually perpendicular P dimers,[37] the amplitude of the RAS signal is a measure for the domain ratio at the GaP/Si(100) surface. The amplitude of the signal measured here (Fig. 3, red line) is as high as for the single-domain GaP/Si(100) reference from Ref. 15. The GaP/Si-As surface is also free of antiphase disorder and exhibits the opposite domain compared to GaP growth on monohydride-terminated Si(100).

In conclusion, we studied Si(100) surface preparation and GaP/Si(100) quasisubstrate growth in MOVPE ambient, which contains As (and Ga, P) residuals, *in situ* with RAS. Both monohydride-terminated and As-modified surfaces were achieved. A two-step annealing process of A-type Si(100) in As results in an As-modified Si(100) surface, which also exhibits a (1×2) surface reconstruction. GaP growth on these As-modified Si(100) substrates results in single-domain epilayers with an inverted sublattice compared to growth on monohydride-terminated Si(100). Growth of single-domain GaP/Si(100) quasisubstrates with the desired sublattice orientation for further processing can thus be obtained in practical growth ambient and in presence of As. Both H and As strongly influence the domain formation on Si(100) which results in a complex III-V/Si interface

formation during nucleation in MOVPE ambient. RAS thereby enables *in situ* control of the entire growth process, and in particular, to prepare well-defined Si surfaces, which is the key to understand the crucial III-V/Si interface formation. Future work is dedicated to the GaP/Si-As heterointerface, which exhibits a more complex atomic structure than GaP/Si-P.

The authors appreciate fruitful discussion with Oleksandr Romanyuk as well as experimental support by Christian Höhn, Antonio Müller, and Matthias Biester. M.M.M., A.N., and A.P. acknowledge Ph.D. scholarships of the Studienstiftung des deutschen Volkes e.V., Carl Zeiss Stiftung, and Landesgraduiertenschule PhotoGrad, respectively. This work was supported by the German Federal Ministry of Education and Research (BMBF, project no. 03SF0525B).

[1] H. Kroemer, J. Cryst. Growth **81**, 193 (1987).
[2] J. Geisz, J. Olson, D. Friedman, K. Jones, R. Reedy, and M. Romero, *Proceedings of the IEEE Photovoltaics Specialists Conference* (IEEE, 2005), Vol. 31, p. 695.
[3] O. Supplie, M. M. May, H. Stange, C. Höhn, H.-J. Lewerenz, and T. Hannappel, J. Appl. Phys. **115**, 113509 (2014).
[4] J. F. Geisz, J. M. Olson, M. J. Romero, C.-S. Jiang, and A. G. Norman, *Proceedings of the 4th IEEE World Conference on Photovoltaic Energy Conversion* (IEEE, 2006), Vol. 1, p. 772.
[5] B. Kunert, I. Németh, S. Reinhard, K. Volz, and W. Stolz, Thin Solid Films **517**, 140 (2008).
[6] S. Brückner, H. Döscher, P. Kleinschmidt, O. Supplie, A. Dobrich, and T. Hannappel, Phys. Rev. B **86**, 195310 (2012).
[7] O. Supplie, M. M. May, C. Höhn, H. Stange, A. Müller, P. Kleinschmidt, S. Brückner, and T. Hannappel, ACS Appl. Mater. Interfaces **7**, 9323 (2015).
[8] S. L. Wright, M. Inada, and H. Kroemer, J. Vac. Sci. Technol. **21**, 534 (1982).
[9] J. M. Olson, M. M. Al-Jassim, A. Kibbler, and K. M. Jones, J. Cryst. Growth **77**, 515 (1986).
[10] N. Dietz, U. Rossow, D. E. Aspnes, and K. J. Bachmann, J. Electron. Mater. **24**, 1571 (1995).
[11] V. K. Dixit, T. Ganguli, T. K. Sharma, S. D. Singh, R. Kumar, S. Porwal, P. Tiwari, A. Ingale, and S. M. Oak, J. Cryst. Growth **310**, 3428 (2008).
[12] I. Németh, B. Kunert, W. Stolz, and K. Volz, J. Cryst. Growth **310**, 1595 (2008).
[13] K. Volz, A. Beyer, W. Witte, J. Ohlmann, I. Németh, B. Kunert, and W. Stolz, J. Cryst. Growth **315**, 37 (2011).
[14] A. Beyer, J. Ohlmann, S. Liebich, H. Heim, G. Witte, W. Stolz, and K. Volz, J. Appl. Phys. **111**, 083534 (2012).
[15] O. Supplie, S. Brückner, O. Romanyuk, H. Döscher, C. Höhn, M. M. May, P. Kleinschmidt, F. Grosse, and T. Hannappel, Phys. Rev. B **90**, 235301 (2014).
[16] O. Supplie, M. M. May, G. Steinbach, O. Romanyuk, F. Grosse, A. Nägelein, P. Kleinschmidt, S. Brückner, and T. Hannappel, J. Phys. Chem. Lett. **6**, 464 (2015).
[17] Y. Kohama, K. Uchida, T. Soga, T. Jimbo, and M. Umeno, Appl. Phys. Lett. **53**, 862 (1988).
[18] R. D. Bringans, D. Biegelsen, and L.-E. Swartz, Phys. Rev. B **44**, 3054 (1991).
[19] L. Kipp, D. Biegelsen, J. Northrup, L.-E. Swartz, and R. D. Bringans, Phys. Rev. Lett. **76**, 2810 (1996).
[20] W. McMahon, I. Batyrev, T. Hannappel, J. Olson, and S. Zhang, Phys. Rev. B **74**, 033304 (2006).
[21] T. Bork, W. McMahon, J. Olson, and T. Hannappel, J. Cryst. Growth **298**, 54 (2007).
[22] T. Hannappel, W. E. McMahon, and J. M. Olson, J. Cryst. Growth **272**, 24 (2004).
[23] T. Hannappel, S. Visbeck, L. Töben, and F. Willig, Rev. Sci. Instrum. **75**, 1297 (2004).
[24] D. E. Aspnes and A. A. Studna, Phys. Rev. Lett. **54**, 1956 (1985).
[25] P. Lautenschlager, M. Garriga, L. Vina, and M. Cardona, Phys. Rev. B **36**, 4821 (1987).
[26] M. Palummo, N. Witkowski, O. Pluchery, R. del Sole, and Y. Borensztein, Phys. Rev. B **79**, 035327 (2009).
[27] S. Visbeck, T. Hannappel, M. Zorn, J.-T. Zettler, and F. Willig, Phys. Rev. B **63**, 245303 (2001).
[28] R. D. Bringans, M. A. Olmstead, R. I. G. Uhrberg, and R. Z. Bachrach, Phys. Rev. B **36**, 9569 (1987).
[29] M. M. May, H.-J. Lewerenz, and T. Hannappel, J. Phys. Chem. C **118**, 19032 (2014).
[30] C. H. Patterson and D. Herrendörfer, J. Vac. Sci. Technol., A **15**, 3036 (1997).
[31] E. S. Tok, A. D. Hartell, and J. Zhang, Appl. Phys. Lett. **78**, 919 (2001).
[32] A. L. Alstrin, P. G. Strupp, and S. R. Leone, Appl. Phys. Lett. **63**, 815 (1993).
[33] A. Paszuk, S. Brückner, M. Steidl, W. Zhao, A. Dobrich, O. Supplie, P. Kleinschmidt, W. Prost, and T. Hannappel, Appl. Phys. Lett. **106**, 231601 (2015).
[34] S. Zollner, M. Garriga, J. Kircher, J. Humlicek, M. Cardona, and G. Neuhold, Phys. Rev. B **48**, 7915 (1993).
[35] L. Töben, T. Hannappel, K. Möller, H. Crawack, C. Pettenkofer, and F. Willig, Surf. Sci. **494**, L755 (2001).
[36] P. H. Hahn, W. G. Schmidt, F. Bechstedt, O. Pulci, and R. del Sole, Phys. Rev. B **68**, 033311 (2003).
[37] H. Döscher and T. Hannappel, J. Appl. Phys. **107**, 123523 (2010).